

# ADVANCES IN CW ION LINACS\*

P.N. Ostroumov<sup>#</sup>

ANL, Argonne, IL 60439, U.S.A.

## Abstract

Substantial research and development related to continuous wave (CW) proton and ion accelerators is being performed at ANL. A 4-meter long 60.625-MHz normal conducting (NC) CW radio frequency quadrupole (RFQ) and a 4K cryomodule with seven 72.75-MHz quarter-wave resonators (QWR) and superconducting (SC) solenoids have been developed, built, commissioned and operated as an upgrade of the CW ion linac, ATLAS, to achieve higher efficiency and beam intensities [1]. Currently we are engaged in development of the first cryomodule for a CW  $H^-$  linac being built at FNAL [2]. This work is well aligned with the development of a 1 GeV 25 MW linac as the driver of a sub-critical assembly for near-term spent nuclear fuel disposal.

The new CW RFQ and cryomodule were fully integrated into ATLAS and have been in routine operation for more than two years and one year, respectively. New design and fabrication techniques for QWRs resulted in the achievement of record accelerating voltages and low cryogenic losses. Since the very beginning the cryomodule provided 17.5 MV accelerating voltage or 2.5 MV per cavity. A 2K cryomodule with eight 162.5-MHz SC half wave resonators (HWR) and eight SC solenoids is being developed for FNAL and scheduled for commissioning in 2017. The testing of the first 2 HWRs demonstrated remarkable performance. Experience with the development and reliable operation of new NC and SC accelerating structures is an essential precursor for the future large scale high power CW accelerators.

## INTRODUCTION

Technology required for both CW RFQ and SC RF accelerators was successfully developed for a recent ATLAS upgrade. This upgrade achieved greater efficiency and beam intensities than were previously obtained at ATLAS and in some cases a 10× improvement is observed [1]. Developments here can be applied to future high-power CW accelerators such as drivers for the production of rare isotope beams or for Accelerator Driven Systems (ADS). In this paper we present the description of major breakthroughs in technologies for CW linacs which have resulted in excellent performance in both normal conducting and SC accelerating structures. Details of our research and developments can be found in numerous conference publications and journal articles published by members of ANL's Physics Division. To save space only key publications will be referenced in this paper.

\*This work was supported by the U.S. Department of Energy, Office of High Energy Physics and Nuclear Physics, under Contract DE-AC02-76CH03000, DE-AC02-06CH11357. This research used resources of ANL's ATLAS facility, which is a DOE Office of Science User Facility.  
<sup>#</sup>ostroumov@anl.gov

## CW ION LINACS

CW linear accelerators can be divided into two main categories: (1) low intensity ion linacs capable of accelerating the majority of ion species from hydrogen to uranium and (2) high intensity light ion linacs, primarily for acceleration of protons and/or deuterons. The linacs in the first category are not affected by the beam space charge and can deliver several hundred kilowatts of beam power; as is the case for FRIB or RAON [3,4]. There are many operational low energy (up to ~25 MeV/u) CW linacs worldwide which are being used for fundamental nuclear physics experiments. Currently, no high-power CW linac exists. Substantial research and development work has been performed in the past decade for several high-power CW linac projects worldwide [2,5-8] and the ability to accelerate several milliamp CW proton beams with SC cavities has been demonstrated in the prototype cryomodule at SARAF [9].

As we discussed in the recent review paper [10], independent of ion species, a CW hadron linac includes a room temperature RFQ accelerator. The transition energy from NC to SC structures depends upon the ion species and the beam intensity. A transition from NC to SC structures is accompanied with significant changes of two main accelerator lattice parameters: (1) the focusing period becomes longer and (2) higher accelerating gradients,  $E_{ACC}$ , are readily achievable when using SC cavities. These changes, if not mitigated, can easily lead to strong coupling of the transverse and longitudinal motions and may result in large emittance growth and beam halo formation. In heavy-ion linacs, the higher accelerating gradients available from SC cavities can be effectively used above ~300 keV/u. In high intensity proton linacs, the transition energy from normal conducting to SC structures must be pushed as high as possible not only to avoid transverse-longitudinal coupling but to suppress space charge effects. Depending on the proton beam current, the transition energy can be in the range from 2 to 7 MeV/u and it is limited by the cost and complexity of CW RFQs.

## CW RFQ

Starting in the 1990's, the ATLAS heavy ion linac included 48 MHz SC resonators capable of accelerating pre-bunched ions with an initial velocity of 0.008c. Due to the high velocity gain in the first 4 SC resonators, a significant distortion of both transverse and longitudinal emittance occurred and resulted in reduced beam transmission through the linac. To address this issue, we have developed and built a CW RFQ capable of accelerating any ion species from 30 keV/u to 295 keV/u. Several innovative ideas have been implemented in this CW RFQ. By selecting a multi-segment split-coaxial

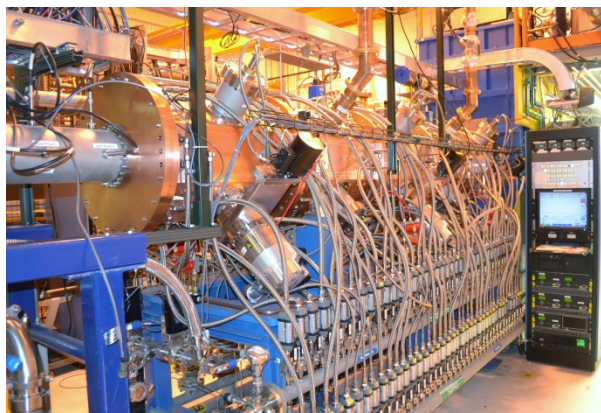


Figure 1: ATLAS front end with the RFQ in position.

structure, we have achieved moderate transverse dimensions for a 60.625 MHz resonator. For the design of the RFQ resonator and vane tip modulations, we have developed a full 3D approach which includes MW-Studio and TRACK simulations of the entire structure [11]. A novel trapezoidal vane tip modulation is used in the acceleration section of the RFQ which resulted in increased shunt impedance. To form an axially symmetric beam exiting the RFQ, a very short output radial matcher, only  $0.75\beta\lambda$  long ( $\beta$  is the particle relative velocity and  $\lambda$  is the RF wavelength), was developed.

Advanced fabrication technology was developed for the construction of the RFQ which included precise machining and two-step high temperature brazing. The RFQ segment was designed to facilitate self-fixturing at the final brazing stage in a large furnace. Thanks to the high accuracy of the overall fabrication, the assembly of the 5-segment RFQ was straightforward and resulted in excellent alignment. The RF measurements found an intrinsic Q equal to 94% of the simulated value for OFE copper. The multi-segment split-coaxial structure creates strong coupling between the quadrants and individual RFQ segments which reduces the effect of local frequency deviations on electromagnetic field distortions. Therefore, no bead-pull measurements were required for tuning of the accelerating field. A high-power water-cooled coupling loop was developed and is based on a cylindrical ceramic window purchased from Kyocera. An important feature of this engineered ceramic window is that the copper cuffs are directly brazed to the ceramic. This feature allowed us to weld the ceramic window directly to the copper parts of the RF coupler, minimizing the heat load. The RF power is delivered to the RFQ from two amplifiers through two RF couplers. The LLRF includes resonance frequency control system which relies on regulating the cooling water temperature of the vanes to phase lock the RFQ to the heavy-ion beams.

The great success of this advanced design and fabrication technology is reflected in the beam parameters measured downstream of the RFQ which are nearly identical to the simulated data [12]. After the successful off-line commissioning, the ATLAS CW RFQ was moved, installed and integrated into the ATLAS system in

December 2012. Fig. 1 shows the current view of the ATLAS front end. Since its inception, the RFQ has provided the acceleration of various ion species spanning the full range of the design charge-to-mass ratio. In addition, the transmission from the Positive Ion Injector (PII) to the experiments is now 100% due to the high quality RFQ beams. Overall reliability of the RFQ system is close to 100%.

It is important to note that during the first 2 years of operation the RFQ RF power transmission system operated without circulators. Circulators were installed about a half year ago and have reduced the number of RF amplifier trips. Further improvements are planned for the RF and cooling system to significantly reduce recovery time after occasional discharges in the RFQ resonator.

## CRYOMODULE DESIGN

In the low energy section of a SC linac, the focusing elements (SC solenoids or SC quadrupoles) can be placed in a common cryostat with the SC cavities. Long drift spaces (as compared to  $\beta\lambda$ ) can amplify the phase and energy errors in the longitudinal phase space. In addition, in high intensity light ion linacs, it is mandatory to have short focusing periods to suppress the space charge effects. Consequently, a long cryomodule design with a high packing factor of SC cavities and focusing elements is essential to preserve the quality of the ion beam at low and medium energies and to reduce project cost.

As we discuss in ref. [10], using SC solenoids for transverse beam focusing together with SC resonators offers several advantages. Therefore, all cryomodules developed at ANL include SC solenoids for the focusing of ion beams.

At Argonne, we have developed a box-type cryomodule which incorporates state-of-the-art techniques such as separate cavity and insulating vacuum systems, stainless steel vacuum vessel with room temperature magnetic shielding and a top-loaded solenoid-cavity string [13]. The first cryomodule for the Proton Improvement Plan II (PIP-II) at FNAL is designed to accelerate the  $H^-$  beam from 2.1 to 11 MeV. To maintain a high beam quality, an adiabatic ramp of the real-estate accelerating gradient is necessary. The cryomodule has eight accelerating-focusing periods with each period containing a 162.5-MHz SC HWR, a SC solenoid for focusing with integrated x-y steering coils, and a beam position monitor. Reduced rf defocusing due to both the low frequency and the small synchronous phase angle results in a much faster energy gain without emittance growth.

The general view of the cryomodule is shown in Fig. 2. The focusing length is 68.6 cm which is adequate for the acceleration of  $\sim 25$  mA beam current. However, PIP-II operational current will be lower by a factor of 10. The HWR cryomodule design incorporates further improvements in alignment accuracy of the cavities and solenoids. A Maxwell kinematic mount will be used to support cavities and solenoids on a long titanium support back machined with high accuracy. We should be

able to provide an accuracy of solenoids and cavity alignment within  $\pm 0.25$  mm peak transversely with  $\pm 0.05^\circ$  for all of the rotation angles.

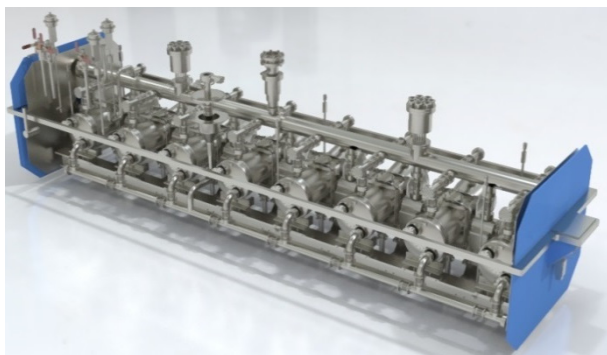


Figure 2: Artistic 3D view of the HWR cryomodule.

## SUPERCONDUCTING CAVITIES

Recently we have developed advanced designs for QWRs and HWRs for application in the low and medium energy sections of CW accelerators. Compared to the previous generation of QWRs and HWRs, several innovations were implemented into the cavity design, fabrication and RF surface treatment [14-17].

### Electromagnetic Design and Optimization

Each type of SC cavity undergoes an extensive electromagnetic optimization procedure to reduce the ratio of the peak electric,  $E_{PEAK}$ , and magnetic,  $B_{PEAK}$ , fields to the accelerating field,  $E_{ACC}$ , simultaneously while maximizing the cryogenic efficiency.  $E_{ACC}$  is defined as the maximum average electric field over the length,  $\beta_{OPT}\lambda$ , for optimal beta. The highly optimized geometries of both the QWR and the HWR are based upon making the outer and inner conductors conical as shown in Fig. 3 for the HWR. The conical design of the cavity allows us to maintain a high packing factor along the beam line while the lateral space can be effectively used to improve cavity electromagnetic (EM) properties.

Another common limitation to the accelerating field is X-ray radiation due to the field emission. At ANL, best practices for RF surface processing and cleaning usually result in  $E_{PEAK} \approx 70$  MV/m with minimal field emission in the ANL QWRs and HWRs. Three additional parameters control the cryogenic efficiency of these cavities, the ratio of shunt impedance,  $R_{SH}$  to the intrinsic quality factor,  $Q_0$ , and geometric factor,  $G = R_S Q_0$ , and the RF surface resistance,  $R_S$ . Both  $R_{SH}$  and  $G$  are design parameters and should be maximized during the electromagnetic optimization of the cavity.  $R_S$  is determined by the SC properties of the cavity niobium material, ambient properties such as external magnetic field and quality of the RF surface processing. We typically achieve  $R_S < 3$  n $\Omega$  at medium fields and with 2 K operation. The main EM parameters of recently built QWRs and HWRs are listed in Table 1.

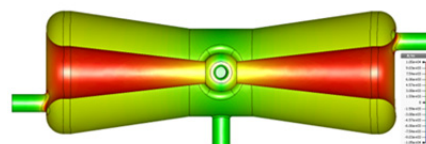


Figure 3: EM model of 162.5 MHz HWR (top), bare niobium cavity with stainless steel flanges (middle) and dressed HWR with slow tuner (bottom).

Table 1: Main Cavity Parameters

Parameter	QWR	HWR
Frequency, MHz	72.75	162.5
Optimal beta	0.077	0.112
Design voltage, MV	2.5	2.0
$E_{PEAK}/E_{ACC}$ , MV/m	5.16	4.7
$B_{PEAK}/E_{ACC}$ , mT/MV/m	7.6	5.0
$G$ , $\Omega$	26	48
$R_{SH}/Q_0$ , $\Omega$	575	271

TEM-class cavities such as QWRs, HWRs and Spoke-loaded cavities can produce multipole components of the electromagnetic field distribution in the accelerating gaps. In recently built QWRs we shape the drift tubes to compensate for dynamic dipole components of the electromagnetic fields. Similarly, for compensation of quadrupole component of the EM fields we developed a “donut” shaped drift tube in the center conductor of the HWR as shown in Fig. 3.

### Mechanical Design and Engineering Analysis

The engineering analysis is usually performed using the ANSYS multiphysics Finite Elemental Analysis (FEA) software. The details of the mechanical design of the cavities and its helium jackets were reported in our previous publications see, for example, ref [18]. The primary tasks of the cavity FEA include: (1) minimization of the resonant frequency sensitivity to the fluctuations of helium pressure,  $\frac{\partial f}{\partial P}$ ; (2) simulations to evaluate the compliance with the pressure vessel code and iteration of the design if necessary; (3) simulations of the slow tuner

operation to provide required tuning range within elastic limits.

### Fabrication

Over the past decade we have developed and established advanced fabrication procedures for TEM-class cavities. Cavity parts are formed from sheet niobium in collaboration with an external vendor AES [19] using various sheet-forming techniques. For the preparation of niobium components for electron beam welding, a wire EDM technique is used instead of traditional machining to reduce the likelihood of inclusions prior to electron-beam welding. The helium jacket is made of 304 stainless steel (SS), therefore, all cavity ports include a braze assembly for transition from niobium ports to SS flanges. Details of fabrication procedures can be found in various conference papers published by the Argonne team over the past 10 years.

### Microphonics

The cavity frequency jitter due to microphonic noise should be minimized for most applications. This is especially valid for low intensity machines where microphonics is the main driver increasing the RF power. There are 2 major techniques to minimize microphonics in QWRs and HWRs: (1) minimize or reduce to zero  $\frac{\partial f}{\partial P}$  by the design of the resonators; (2) mechanically adjust the inner conductor to position it in the electromagnetic center of the cavity. Finding the electromagnetic center is equivalent to finding the highest resonant frequency while the drift tube position is slightly displaced mechanically both longitudinally and laterally [20,21]. QWRs are susceptible to the microphonics due to pendulum-like motion of the long central conductor, therefore mechanical dampers are also effective in the QWRs [21].

### Surface Processing

The mechanics of electropolishing QWRs and HWRs, where the center conductor and outer conductor are coaxial, is somewhat similar to the highly optimized procedure for polishing elliptical cell cavities for the ILC. ANL has the unique capability to perform electropolishing on complete QWRs and HWRs with the integral helium jacket installed [22].

### Performance Test

The majority of jacketed and electropolished cavities undergo cold testing at 2K and 4K in a test cryostat prior to the installation into the cryomodule. A combination of innovative advanced design, fabrication and RF surface processing techniques resulted in excellent performance for both the QWRs and the HWRs. Typically, these cavities can operate at peak surface electric fields up to 70 MV/m without significant X-rays. At 2K, the residual resistance of these cavities is below 2.5 n $\Omega$  at 60 MV/m peak electric field, which corresponds to ~70 mT peak magnetic field. Four 72.75 MHz QWRs out of seven were cold tested in the test cryostat and all of them provided at

least 4.0 MV voltage,  $E_{PEAK} > 70$  MV/m and  $B_{PEAK} > 105$  mT [16,17,23].

## SUB-SYSTEMS

### RF Coupler and Slow Tuner

Both QWRs and HWRs are equipped with a double-window multi-kW adjustable capacitive RF input coupler. Nitrogen or helium gas cools the cold window. The design and performance of the RF input coupler was discussed elsewhere [24]. 4-kW adjustable RF couplers are being operated in the new ATLAS cryomodule since January 2014. A similar RF coupler rated for up to 10 kW at 162 MHz has been developed and tested for the HWRs.

A pneumatically actuated mechanical slow tuner which compresses the cavity along the beam axis is located outside of the helium vessel and it is attached to the SS flanges as shown in Fig. 3. Currently we are developing improved design of slow tuners to substantially increase operational reliability for application in the FRIB driver linac.

Due to low microphonic noise, 3-4 kW RF power per cavity is sufficient for phase-locked operation. There is no need for a fast tuner.

### SC Solenoids

The conceptual design of a magnet assembly which includes main solenoid coil, bucking coils and dipole coils for beam steering corrections in both horizontal and vertical planes was developed a while ago [25]. The bucking coils substantially cancel the stray field such that magnets may be installed next to the SC cavities without any magnetic shielding. Such a magnet assembly was built for the FNAL proton driver and cold tested together with a HWR with relative locations of the devices similar to that for operations. We observed that the quality factor of the cavity does not change even after the cavity is quenched in the presence of magnetic field generated by the solenoid and dipole coils [26]. The magnet assemblies with bucking coils (but without dipole coils) were installed in the new ATLAS cryomodule and are being successfully operated.

## QWR CRYOMODULE COMMISSIONING

The seven QWRs and four SC solenoids were installed in the new cryomodule in 2013. The clean hermetic assembly of the cavity-solenoid string was completed in a cleanroom and then transferred and hung from the bottom of the cryostat lid where the final alignment of the resonators and solenoids and other “dirty” work was continued. After off-line cold and RF testing, the cryomodule was installed into ATLAS and cooled down in December 2013. Figure 4 shows loading of the assembled cavity-solenoid string into the box cryostat in the accelerator tunnel. The static heat load was measured to be just 12 Watts [27]. Beam commissioning of the new beam-lines and new cryomodule was completed in March 2014. The effective cavity voltage was calculated by fitting TRACK simulations to the measured energy gain.

The total effective voltage of the cryomodule is 17.5 MV, or 2.5 MV per cavity on average. As discussed in ref. [1,28], all cavities are capable of providing at least a 3.75 MV voltage.

Currently, the available cavity voltage is limited by the LLRF system. The stability of the LLRF system at higher fields will be investigated as time permits during brief periods of ATLAS maintenance.



Figure 4: Cold mass assembly loading into the cryostat vacuum vessel in the tunnel.

## APPLICATIONS

The experience gained with the developments of CW RFQ, new QWRs and HWRs can be directly applied to the design of a high power CW driver linac for nuclear waste transmutation or ADS. No significant R&D is required to proceed with a 1 GeV, 25 mA linac design and construction. An area which requires some R&D is the development of high power RF input couplers [29].

We have developed preliminary physics design for a 25 MW proton driver [30]. The linac includes a 3 MeV RFQ operating at a fundamental frequency of 162.5 MHz. Five types of SC cavities (Fig. 5) are required to cover full energy range. 121 SC cavities and 55 SC solenoids are housed in 19 cryomodules. The total length of the linac is 150 meters.

A preliminary physics design and simulations indicate that a 25 mA beam can be accelerated without beam halo

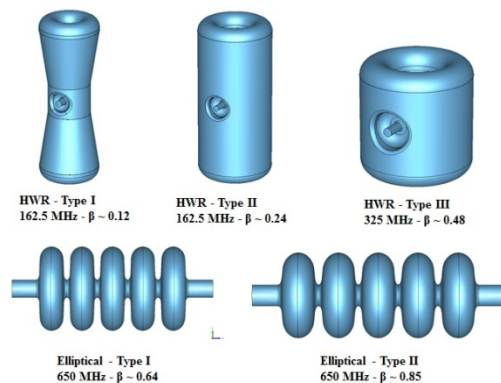


Figure 5: Types of cavities designed for the ADS linac at different  $\beta$  values and frequencies.

formation and, consequently, beam losses. More detailed optimizations are required for the low-energy section and the transverse beam dynamics prior the final design of the linac.

## SUMMARY

This paper reports advanced technologies for both normal conducting and superconducting accelerating structures developed at ANL for application in CW hadron linacs. A CW RFQ providing high quality ion beams has been in operation for several years with high reliability. The performance of the QWRs and HWRs is remarkable and sets a new world record both in terms of accelerating gradients and residual resistance. Limited R&D is required for the development and construction of a 25 MW driver linac for ADS or for transmutation of spent nuclear fuel.

## ACKNOWLEDGMENT

I would like to thank my colleagues from Physics, High Energy Physics and Nuclear Engineering Divisions at ANL and our collaborators from FNAL, Advanced Energy Systems and Meyer Tool for significant contributions to this work.

## REFERENCES

- [1] P.N. Ostroumov et al, LINAC-14, p. 449.
- [2] V.A. Lebedev, Paper MOPMA014, these Proceedings.
- [3] J. Wei et al., IPAC-14, p. 17.
- [4] D. Jeon, LINAC-14, p. 775.
- [5] R. Ferdinand et al., SRF-13, p. 11.
- [6] A. Mosnier, LINAC-08, p. 1114.
- [7] S. Fu et al., SRF-11, p. 977.
- [8] J.-L. Biarrotte et al., SRF-13, p. 129.
- [9] D. Berkovits et al, LINAC-12, p.100.
- [10] P.N. Ostroumov and F. Gerigk, Rev. of Acc. Science and Technology, January 2013, Vol. 06, p. 171.
- [11] B. Mustapha, A.A. Kolomiets and P.N. Ostroumov, Phys. Rev. ST Accel. Beams 16, 120101 (2013).
- [12] P.N. Ostroumov et al., Phys. Rev. ST-AB 15, 110101/1-11 (2012).
- [13] J. Fuerst, SRF-09, p. 52.
- [14] B. Mustapha, P.N. Ostroumov, LINAC-2010, p. 169.
- [15] B. Mustapha et al., IPAC-12, p. 2289.
- [16] M.P. Kelly, Reviews of Accelerator Science and Technology, Volume 5 (2012), pp. 185-203.
- [17] Z.A. Conway, M.P. Kelly and P.N. Ostroumov, Nucl. Instrum. Methods Phys. Res. B 350, 94 (2015).
- [18] P.N. Ostroumov et al., SRF-11, p.132.
- [19] <http://www.aesys.net/>
- [20] Z.A. Conway, Slides, SRF-11, p. 943.
- [21] M.P. Kelly et al., LINAC-12, p. 348.
- [22] S.M. Gerbick et al., SRF-11, p. 576.

Content from this work may be used under the terms of the CC BY 3.0 licence (© 2015). Any distribution of this work must maintain attribution to the author(s), title of the work, publisher, and DOI.

- [23] Z.A. Conway, LINAC-14, p. 46.
- [24] M.P. Kelly et al., LINAC-12, p. 678.
- [25] P.N. Ostroumov et al., LINAC-02, p. 64.
- [26] S. Kim et al., Paper WEPTY009, these Proceedings.
- [27] Z.A. Conway et al., LINAC-14, p. 437.
- [28] M.P. Kelly et al., LINAC-14, p. 440.
- [29] S.V. Kutsaev et al., SRF-13, p. 1055.
- [30] B. Mustapha et al., LINAC-14, p. 52.